# Rearrangement in a Tripodal Nitroxide Ligand To Modulate the Reactivity of a Ti−F Bond

Michael A. Boreen, Justin A. Bogart, Patrick J. Carroll, and Eric J. Schelter*

P. Roy and Diana T. Vagelos Laboratories, Department of Chemistry, University of Pennsylvania, 231 South 34th Street, Philadelphia, Pennsylvania 19104, United States

S *Supporting Information*

ABSTRACT: The tripodal nitroxide ligand $[(2\text{-}^tBuNO)\text{-}C_6H_4CH_2)_3N]^{3-}$ (TriNOx^{3-}) binds the Ti(IV) cation and prevents inner-sphere coordination of chloride in the complex $[Ti(TriNOx)]Cl$ (**1**). The ligand undergoes an η^2-NO to κ^1-O rearrangement to enable a fluoride ion to bind in the related complex Ti(TriNOx)F (**2**). Computational and reactivity studies demonstrated that the ligand rearrangement contributed to the enthalpy change in the transfer of a fluoride anion.
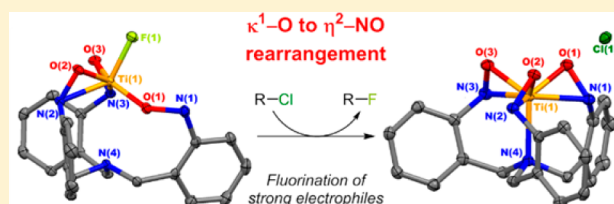

INTRODUCTION

New methods of fluorinating small molecules are critical to modern chemical industries. Approximately 20% and 30% of pharmaceutical and agricultural compounds, respectively, contain fluorine atoms.[1,2] Late-stage fluorination chemistries are of particular interest, as these methods expand the synthetic routes available for the synthesis of pharmaceuticals and agrochemicals and afford better ways to synthesize ^{18}F positron emission tomography (PET) tracers.[3,4] It is of interest to develop simple and selective nucleophilic fluorination procedures.

Ideal fluoride sources are soluble in organic solvents. Considering metal-based sources, the fluoride salts KF, CsF, and AgF are common nucleophilic fluoride sources but have limitations due to poor solubility. Recently, our group reported the first example of a organo-cerium(IV) fluoride complex[5] as part of a broader interest in the coordination chemistry of metal fluorides and fluoride-containing ligands.[6−8] In the current contribution, an η^2-NO to κ^1-O rearrangement process in a multidentate nitroxide ligand was shown to increase the reactivity of a Ti^{IV}−F moiety due to steric pressure at the metal cation and a favorable enthalpy change upon rearrangement of the ligand arm from a κ^1-O to η^2-NO coordination mode.

Recently, our group showed that the coordination chemistry of the tripodal nitroxide ligand $[(2\text{-}^tBuNO)C_6H_4CH_2)_3N]^{3-}$ (TriNOx^{3-}) (Figure 1) with a series of rare-earth ions was highly dependent upon cation size.[9] Since Ti(IV) is smaller than the rare-earth ions, we expected TriNOx^{3-} would form a sterically hindered Ti(IV) complex. Herein, we demonstrate that the TriNOx^{3-} framework undergoes a change in coordination mode depending on anion size at the Ti(IV) cation.
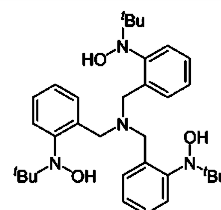
Figure 1. H$_3$TriNOx.

RESULTS AND DISCUSSION

Synthesis and Characterization of Complexes. The complex $[Ti(TriNOx)]Cl$ (**1**) was synthesized in 53% yield by adding a THF solution of H$_3$TriNOx and Et$_3$N to a−78 °C THF solution of TiCl$_4$(THF)$_2$ (Scheme 1). Complex **1** was air-

Scheme 1. Synthesis of $[Ti(TriNOx)]Cl$ (1)
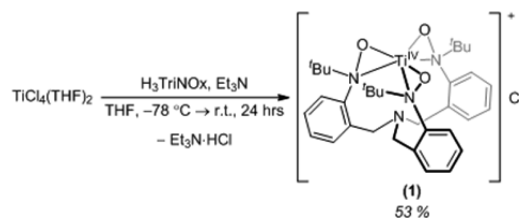
and water-stable and water-soluble. High-resolution mass spectrometry showed the presence of the $[Ti(TriNOx)]^+$ cation. Cooling a saturated DCM solution of **1** to −78 °C yielded X-ray-quality yellow crystals, enabling determination of the solid-state structure (Figure 2).

Figure 2. Thermal ellipsoid plot of **1** at the 50% probability level with hydrogen atoms and ^{t}Bu groups omitted for clarity. Selected bond distances (Å): Ti(1)−O(1) 1.8912(14), Ti(1)−O(2) 1.8720(13), Ti(1)−O(3) 1.8900(14), Ti(1)−N(1) 2.1682(17), Ti(1)−N(2) 2.1852(16), Ti(1)−N(3) 2.1959(16), Ti(1)−N(4) 2.2775(16), N(1)−O(1) 1.440(2), N(2)−O(2) 1.436(2), N(3)−O(3) 1.441(2).
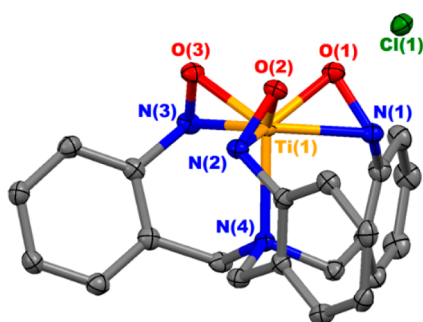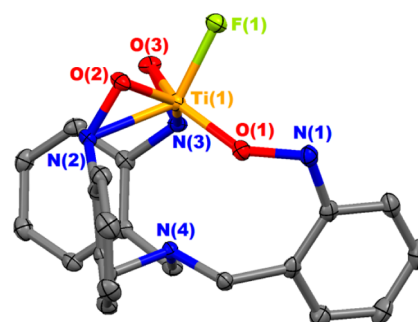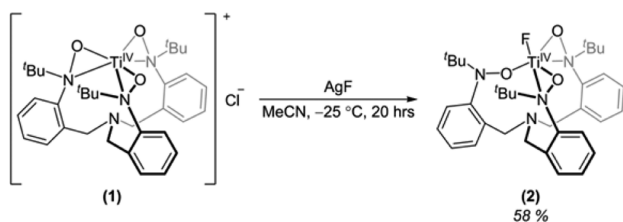

Figure 3. Thermal ellipsoid plot of **2** at the 50% probability level with hydrogen atoms and ^{t}Bu groups omitted for clarity. Selected bond distances (Å): Ti(1)−F(1) 1.8536(11), Ti(1)−O(1) 1.8017(14), Ti(1)−O(2) 1.8857(14), Ti(1)−O(3) 1.8929(14), Ti(1)−N(2) 2.1937(16), Ti(1)−N(3) 2.2458(16), N(1)−O(1) 1.400(2), N(2)−O(2) 1.4278(19), N(3)−O(3) 1.444(2).

The crystal structure of **1** showed that the chloride ion was outer sphere, leaving an ion-paired, effectively C_3 symmetric [Ti(TriNOx)]$^+$ cation in the solid state. Evidently due to coordination through three η^2-NO groups, the titanium center was too sterically encumbered to accommodate a chloride ligand. The related homoleptic compounds Ti(ONMe$_2$)$_4$[10] and Ti(ONEt$_2$)$_4$[11] were reported to be eight-coordinate, with four η^2-NO groups in each case. The average Ti−O bond length of 1.844(14) Å in **1** was shorter than those in Ti(ONMe$_2$)$_4$ (average 1.947(1) Å)[10] and Ti(ONEt$_2$)$_4$ (1.980(3) Å).[11] The average Ti−N(nitroxide) bond length in **1** was 2.1831(16) Å, slightly longer than those of Ti(ONMe$_2$)$_4$ (average 2.1625(1) Å)[10] and Ti(ONEt$_2$)$_4$ (2.108(5) Å).[11] The average N−O bond length of 1.439(2) Å in **1** was slightly longer than those in Ti(ONMe$_2$)$_4$ (average 1.428(1) Å)[10] and Ti(ONEt$_2$)$_4$ (1.402(7) Å).[11] Bond distances and NMR spectra (Figures S1 and S2 in the Supporting Information) for **1** are consistent with a Ti(IV) cation bonded to three fully reduced nitroxide groups.[10−19]

We hypothesized that the TriNOx$^{3−}$ ligand could change its coordination mode to accommodate an additional ligand at the titanium center. With this concept in mind, we targeted the small, negatively charged fluoride ion. Indeed, the reaction of complex **1** with AgF in −25 °C acetonitrile overnight caused X-ray-quality orange crystals of Ti(TriNOx)F (**2**) to form (Scheme 2, and Figure 3). The crystal structure of complex **2**

Scheme 2. Synthesis of Ti(TriNOx)F (2) from Complex 1

confirmed the hypothesis that TriNOx$^{3−}$ could undergo structural rearrangement in order to accommodate another ligand at the titanium center. A comparison of the structures of **1** and **2** (Figures 2 and 3) showed that one of the η^2-NO nitroxide groups in complex **1** switched to κ^1-O coordination in complex **2**. The Ti(1)−O(1) and N(1)−O(1) bond lengths in the structure of **2**, 1.8017(14) and 1.400(2) Å, respectively, were consistent with a reduced, anionic nitroxide group,[10−19]

indicating that the κ^1-O-bound nitroxide group was not oxidized. The NMR spectra of **2** (Figures S3−S5 in the Supporting Information) were also consistent with this assignment. Additionally, the distance from the titanium cation to the apical nitrogen, N(4) in Figures 2 and 3, increased from 2.2775(16) Å in **1** to 3.073(1) Å in **2**. Majumdar and co-workers reported the lengthening and concurrent weakening of the V−N$_{axial}$ bond when V(III) complexes of tris(2-aminoethyl)amine (tren) derivatives were converted to their respective V^V−oxo complexes.[20] Lengthening or dissociation of the apical nitrogen in tripodal ligand frameworks can be a significant thermodynamic factor when an additional ligand bonds to the metal cation.[20] Both of the observed structural changes in the TriNOx$^{3−}$ ligand opened the coordination sphere, allowing the fluoride to bind the titanium cation.
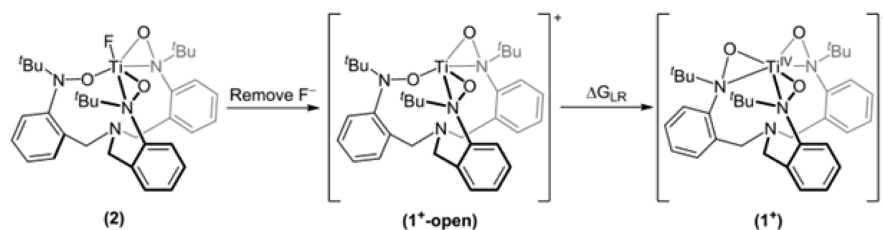
To compare the sterics of the TriNOx$^{3−}$ ligand in complexes **1** and **2** quantitatively, the program SambVca was used to calculate the percent buried volume (%V_{Bur}) for each complex.[21] Percent buried volume values have primarily been used to examine the steric demand of phosphines and NHCs,[22] but they have also been applied to a variety of ligands, including guanidinates,[23] aryloxides,[24] and 1,4,7-triazacyclononanes.[25] We calculated %V_{Bur} values of 92.8% for TriNOx$^{3−}$ in **1** and 82.0% for TriNOx$^{3−}$ in **2** (see the Experimental Section for full details). Thus, the change in coordination mode of TriNOx$^{3−}$ changed its steric profile significantly, consistent with the coordination of a fluoride ligand in complex **2**.

Solution-phase cyclic voltammetry experiments were performed to assess the differences in electronic properties between complexes **1** and **2** (Figures S8−S10 in the Supporting Information). Complex **1** exhibited a ligand-based, quasi-reversible redox couple with E_{pc} = 0.58 V versus ferrocene and E_{pa} = 0.36 V and a chemically irreversible titanium reduction feature with E_{pc} = −1.67 V. Complex **2** exhibited two ligand-based irreversible oxidation features at E_{pa} = −0.28 and 0.23 V and an irreversible metal reduction feature at E_{pc} = −1.89 V. As expected, the electron-donating fluoride ligand stabilized the redox features on complex **2** to more negative potentials. The shift in the potential of the ligand oxidation had important synthetic repercussions, since the reduction potential of Ag$^+$ in acetonitrile is 0.04 V versus ferrocene.[26] In solution at room temperature, complex **2** was observed to be oxidized rapidly by silver(I) salts. Solvent and temperature were thus important aspects of the synthesis of **2**; isolation of **2** was enabled by its precipitation from solution before reaction with Ag$^+$.

Scheme 3. Computational Scheme Used To Calculate the ΔG Value of Ligand Rearrangement (ΔG$_{LR}$)

Reactions of **1** with CsF in acetonitrile at room temperature also led to formation of **2**, but the product decomposed under these conditions, preventing its isolation in good yield. We avoided using common acidic fluoride sources such as Et$_3$N(HF)$_3$ and pyridine(HF) to synthesize **2**, as the presence of free H$_3$TriNOx in some reactions with **2** suggested that **2** was sensitive to acidic protons. BF$_3$·Et$_2$O was also not used due to concerns it would react further by abstracting the fluoride ligand from **2** to form the BF$_4^-$ salt. Complex **1** reacted only slowly with CsF in acetonitrile at −25 °C, giving very low yields of **2**. This result suggested that reactions with other poorly acetonitrile-soluble fluorides, such as [Me$_4$N]F, would not be productive for synthesizing **2**. At room temperature and at −25 °C, **1** reacted with AgF much more quickly than with CsF. The high reactivity of AgF was evidently important for the reaction to occur at −25 °C; under the same conditions, the reaction with CsF was too slow to achieve a reasonable yield. AgF, AgCl, and **2** were all insoluble in −25 °C acetonitrile; thus, once **2** formed, it precipitated as crystals that were not oxidized by the silver salts also present. On the other hand, the solubility of **1** under these conditions allowed the reaction to occur despite not having AgF in solution. The combination of the solubility of **1** and the lack of solubility of AgF, AgCl, and **2** under the reaction conditions were thus all key for the reaction to occur but without the product decomposing.

^{19}F NMR spectroscopy supported the claim that the fluoride ion was inner sphere in solution. The ^{19}F chemical shift of **2** was 114.6 ppm in CD$_2$Cl$_2$, while free fluoride ions (from tetramethylammonium fluoride) in CH$_2$Cl$_2$ appeared at −97 ppm.[27] The reported ^{19}F chemical shifts of (C$_5$H$_4$Me)TiF$_3$[28] and {[Me$_2$Si(C$_5$H$_4$)$_2$]TiF$_2$}[29] in CDCl$_3$ were 131.0 and 68.8 ppm, respectively. The ^{1}H and ^{13}C NMR spectra of **1** and **2** were similar; both sets of data indicated a C_3-symmetric complex (Figures S1−S4 in the Supporting Information). The [Ti(TriNOx)]$^+$ cation of **1** was expected to show C_3 symmetry, but the NMR data for **2** were unexpected, on the basis of the rearrangement of one nitroxide arm in the solid-state structure. A gas-phase geometry optimization of **2** predicted a minimum energy structure close to that shown in Figure 3 (vide supra), showing that the results of the calculations were consistent with the asymmetric coordination mode observed in the solid state. However, the NMR data indicated that **2** was symmetric in solution at 300 K with the three nitroxide groups rapidly interconverting between the η^2-NO and κ^1-O coordination modes. Variable-temperature ^{1}H and ^{19}F NMR experiments on **2** in CD$_2$Cl$_2$ showed that the spectra retained C_3 symmetry to 200 K (Figures S6 and S7 in the Supporting Information). Thus, the energetic barrier to this fluxional process was small.

Computational Studies of Complexes. An important consequence of these observations was that the higher energy conformation of TriNOx$^{3−}$ would be expected to destabilize the fluoride ligand, as loss of the fluoride ligand would allow the

TriNOx$^{3−}$ ligand to return to a lower energy conformation. In an initial reactivity experiment, complex **2** was reacted with (CH$_3$)$_3$SiCl in CDCl$_3$, resulting in instant, nearly quantitative conversion to **1** and (CH$_3$)$_3$SiF. Since we had shown **2** could perform fluorination chemistry and cleanly return to **1**, we decided to perform computational studies of fluorination with **2** (see the Supporting Information for full details).

DFT calculations were performed at the B3LYP level of theory with the 6-31G* basis set; calculations with solvent continuum were performed using the CPCM SCRF method. Complexes **2** and **1$^+$** (**1$^+$** = [Ti(TriNOx)]$^+$) were optimized in each solvent continuum on the basis of crystal structures or calculated gas-phase coordinates. Complex **1$^+$-open** represented complex **2** with the fluoride ion removed, and it was not optimized (Scheme 3). Complex **1$^+$-open** had the same number of atoms and charge as complex **1$^+$** but had the TriNOx$^{3−}$ ligand in the same conformation as in complex **2**, enabling comparison of the free energy of TriNOx$^{3−}$ in each conformation at the Ti(IV) cation (Scheme 3).

On the basis of Scheme 3, ΔG$_{LR}$, the free energy of ligand rearrangement, was calculated in the gas phase and in benzene, chloroform, and acetonitrile by subtracting the total free energy of **1$^+$-open** from the free energy of **1$^+$**. ΔG$_{LR}$ approximated the energy difference between the two TriNOx$^{3−}$ coordination modes. The heterolytic Ti−F bond strength was estimated by subtracting the free energy of **2** from the sum of the free energies of **1$^+$** and a fluoride anion.

The calculated ΔG$_{LR}$ values in each solvent continuum are shown in Table 1. The negative values of ΔG$_{LR}$ indicated that

Table 1. Calculated ΔG$_{LR}$ Values and Heterolytic Ti−F bond Strengths^a

	gas phase	solution		
		C$_6$H$_6$	CHCl$_3$	CH$_3$CN
ΔG$_{LR}$ (kJ/mol)	−179.7	−151.7	−135.8	−121.6
heterolytic Ti−F bond strength (kJ/mol)	754.3	474.6	365.5	277.1

^{a}Calculated free energies of **1$^+$**, **1$^+$-open**, and **2** in each solvent appear in Table S1 in the Supporting Information.
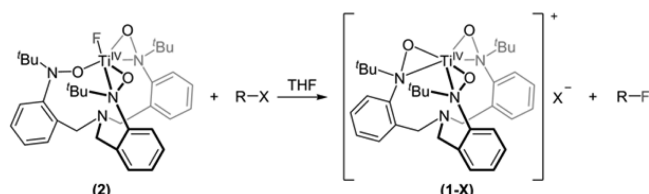
1$^+$ was more stable than **1$^+$-open**, as expected. ΔG$_{LR}$ increased from −179.7 kJ/mol in the gas phase to −121.6 kJ/mol in acetonitrile as the solvent polarity increased. As expected, the heterolytic Ti−F bond strength was weaker in more polar solvents. On the basis of our calculations, the ligand rearrangement energy change was comparable to that of heterolytic cleavage of the Ti−F bond in acetonitrile and amounted to a significant contribution to fluorine transfer reactions with **2**.

For comparison we calculated the heterolytic Ti−F bond strength of the azatitanatrane [(HNCH$_2$CH$_2$)$_3$N]TiF.[30] Calcu-

lations showed that this system exhibited only very minor ligand rearrangement after removal of the fluoride ion and optimization of $\{[(HNCH_2CH_2)_3N]Ti\}^+$, mainly due to shortening of the Ti−N bonds. By the same method used to calculate the values in Table 1 (see the Supporting Information for full details), the heterolytic Ti−F bond strength of $[(HNCH_2CH_2)_3N]TiF$ was calculated to be 992.6 kJ/mol in the gas phase, almost 250 kJ/mol larger than that in complex **2**. This result supported the hypothesis that ligand rearrangement between **2** and **1** contributed to the heterolytic Ti−F bond scission.

Fluorine Transfer Reactions with Ti(TriNOx)F. On the basis of the instantaneous reaction of **2** with $(CH_3)_3SiCl$ to form $(CH_3)_3SiF$ in 98% yield (entry 1, Table 2), we decided to

Table 2. Fluorine Transfer Reactions with 2[a]

entry	substrate	temp (°C)	time	conversn (%)[b]
1	$(CH_3)_3SiCl$[c]	23	5 min[d]	98
2	$[Ph_3C][PF_6]$[e]	23	5 min[d]	42
3	Ph_3CBr	60	1 h	98
4	Ph_3CCl	60	24 h	dec[f,h]
5	^tBuBr	60	24 h	dec[g,h]
6	$PhCOCl$	60	1 h	18
7	$4\text{-}(CH_3)\text{-}C_6H_4SO_2Cl$	60	2 h	4

[a]Reactions were performed in a sealed J-Young NMR tube with 10 mg of complex **2** and 2 equiv of the substrate, unless specified otherwise. [b]Percent conversion from ^{19}F NMR with PhF internal standard. [c]Substrate was added in air. [d]The reaction was complete instantly. [e]1.4 equiv of substrate. [f]81% of **2** remained after 24 h. [g]41% of **2** remained after 24 h. [h]90% of **2** remained after 24 h at 60 °C without substrate.

investigate the scope of fluorine transfer reactions with **2** in THF (see the Experimental Section for details of fluorine transfer reaction procedures). Complex **2** was initially reacted with 1-iodobutane, benzyl chloride, and 4-nitrobenzyl bromide, substrates ideal for associative reaction pathways. However, no fluorine-transfer products were observed in these cases. We then elected to react **2** with $[Ph_3C][PF_6]$ (entry 2), an ideal substrate for dissociative chemistry, as it acts as a source of the trityl carbocation. A precipitate, presumably $[Ti(TriNOx)]\text{-}[PF_6]$, formed instantly from this reaction, and ^{19}F NMR showed 42% conversion to Ph_3CF. No other products were observed by ^{19}F NMR; it remains unclear what other products were formed. Complex **2** reacted cleanly with Ph_3CBr at 60 °C, giving 98% conversion to Ph_3CF (entry 3). However, complex **2** slowly decomposed with no conversion to the fluorinated product on reaction with Ph_3CCl or ^tBuBr at 60 °C (entries 4 and 5, respectively). These results indicated that the generation of a carbocation was necessary for **2** to fluorinate an alkyl halide.

Poor yields of the corresponding fluorinated products were obtained when **2** was reacted with $PhCOCl$ and $4\text{-}(CH_3)\text{-}C_6H_4SO_2Cl$ (Table 2, entries 6 and 7, respectively). These fluorination reactions indicated that the Ti−F bond of **2** could only be broken using highly electrophilic molecules. An

additional factor that drove the Ti−F bond cleavage was precipitation of $[Ti(TriNOx)]X$ ($X = Br^-, Cl^-, PF_6^-$) in THF.

Fluorination reactions with titanium−fluoride complexes and organic substrates are uncommon in the literature, although examples of C−F bond activation with titanium complexes and organofluorine compounds have been reported.[29,31−35] There are also many examples of reactions with organosilicon substrates.[31,36−39] Taw et al. reported reaction of $Cp_2Ti(CF_3)\text{-}(F)$ with 5 equiv of $(CH_3)_3SiCl$ to form $Cp_2Ti(CF_3)(Cl)$. In contrast, **2** instantly reacted with $(CH_3)_3SiCl$ to completion. Thus, while the high Ti−F bond strength disfavored fluoride transfer, the high-energy conformation of $TriNOx^{3-}$ in **2** increased the reactivity of the fluoride.

■ CONCLUSIONS

Two complexes of titanium with a tripodal nitroxide ligand were synthesized. Percent buried volume calculations confirmed that ligand rearrangement upon replacing the chloride counterion with fluoride permitted coordination of the fluoride ligand to the titanium center. DFT calculations supported the hypothesis that the ligand rearrangement stored energy, providing driving force for fluorine transfer reactions. Reactivity studies confirmed that the titanium fluoride complex could rapidly fluorinate highly electrophilic substrates. On the basis of these results, high-energy ligand rearrangements may contribute to new strategies for the development of fluoride transfer reagents.

■ EXPERIMENTAL SECTION

General Methods. Unless otherwise noted, all reactions and manipulations were performed under an inert atmosphere (N_2) using standard Schlenk techniques or in a Vacuum Atmospheres, Inc. Nexus II drybox equipped with a molecular sieve 13X/Q5 Cu-0226S catalyst purifier system. Glassware was oven-dried for at least 3 h at 150 °C prior to use. ^1H and ^{13}C NMR spectra were obtained on a Bruker DMX-300 Fourier transform NMR spectrometer at 300 and 75.4 MHz, respectively. ^{19}F NMR spectra were obtained on a Bruker DMX-300 or DMX-360 Fourier transform NMR spectrometer at 282.2 or 338.7 MHz, respectively. Chemical shifts were recorded in units of parts per million (for ^1H and ^{13}C spectra) downfield from residual solvent signals or (for ^{19}F spectra) referenced to an external $CFCl_3$ reference at 0 ppm, an internal fluorobenzene standard at −113.15 ppm (for fluorine transfer reactions), or an internal hexafluorobenzene standard at −164.9 ppm (for variable-temperature NMR). All coupling constants were reported in Hz. ^1H and ^{19}F variable-temperature NMR measurements were carried out at 300 and 282 MHz, respectively. Infrared spectra were obtained from 400 to 4000 cm^{-1} using a PerkinElmer Spectrum 100 FT-IR spectrometer. High-resolution mass spectra were measured using a Waters 2695 Separations Module (1S0RR23444).

Materials. Tetrahydrofuran, acetonitrile, hexanes, diethyl ether, fluorobenzene, and dichloromethane were purchased from Fisher Scientific. The solvents were sparged for 20 min with dry N_2 and dried using a commercial two-column solvent purification system comprising columns packed with Q5 reactant and neutral alumina, respectively (for hexanes), or two columns of neutral alumina (for THF, Et_2O, CH_2Cl_2, fluorobenzene, and CH_3CN). Deuterated solvents were purchased from Cambridge Isotope Laboratories, Inc., and stored over 4 Å molecular sieves for several days prior to use. $H_3TriNOx$,[9] $TiCl_4(THF)_2$,[40] and the supporting electrolyte $[^nPr_4N][B(3,5\text{-}(CF_3)_2\text{-}C_6H_3)_4]$[41] were prepared according to literature procedures. All other materials were purchased from commercial sources. Triethylamine (Et_3N) was used after three freeze−pump−thaw cycles. Benzyl chloride and hexafluorobenzene were distilled under vacuum and used after three freeze−pump−thaw cycles. 2-Bromo-2-methylpropane (^tBuBr) was washed with $CaCl_2$ and K_2CO_3 and dried over molecule

sieves after three freeze−pump−thaw cycles prior to use. Benzoyl chloride (PhCOCl) was washed with $CaCl_2$ and dried over molecular sieves after three freeze−pump−thaw cycles prior to use. 1-Iodobutane was washed with $MgSO_4$ and filtered through activated alumina after three freeze−pump−thaw cycles prior to use. 4-Methylbenzenesulfonyl chloride (4-(CH_3)-$C_6H_4SO_2Cl$) and ferrocene (Fc) were sublimed under vacuum at 80 and 23 °C, respectively, prior to use. Cesium fluoride (CsF) was dried under vacuum at 90 °C prior to use. Silver fluoride (AgF), trimethylsilyl chloride (($CH_3)_3SiCl$), 4-nitrobenzyl bromide, triphenylmethyl bromide (Ph_3CBr), triphenylmethyl chloride (Ph_3CCl), and triphenylmethyl hexafluorophosphate ($[Ph_3C][PF_6]$) were used as received.

General Procedure for Fluorine Transfer Reactions. In a J. Young NMR tube was placed a protio THF solution of ∼10 mg of complex **2** and fluorobenzene as an internal standard. An initial ^{19}F NMR spectrum was recorded, and then the corresponding substrate was added under N_2. The reaction was monitored by ^{19}F NMR spectroscopy and was considered complete when the signal at 163 ppm (the position of the ^{19}F resonance of **2** in THF) disappeared completely. Percent conversion values were calculated on the basis of integration of the product against the internal standard.

Electrochemistry. Cyclic voltammetry (CV) experiments were performed using a CH Instruments 620D Electrochemical Analyzer/Workstation, and the data were processed using CHI software v 9.24. All experiments were performed in an N_2 atmosphere drybox using electrochemical cells that consisted of a 4 mL vial, glassy-carbon (3 mm diameter) working electrode, a platinum-wire counter electrode, and a silver wire plated with AgCl as a quasi-reference electrode. The working electrode surfaces were polished prior to each set of experiments and were periodically replaced on scanning >0 V versus ferrocene (Fc) to prevent the buildup of oxidized product on the electrode surfaces. Potentials were recorded in CH_2Cl_2 and were referenced versus Fc, which was added as an internal standard for calibration at the end of each run. Solutions employed during CV studies were ∼3 mM in analyte and 100 mM in $[^nPr_4N][B(3,5-(CF_3)_2-C_6H_3)_4]$ ($[^nPr_4N][BAr^F_4]$). All data were collected in a positive-feedback IR compensation mode. The CH_2Cl_2 solution cell resistances were measured prior to each run to ensure resistances ≤∼500 Ω.[41] Scan rate dependences of 50−1000 mV/s were performed to determine electrochemical reversibility.

X-ray Crystallography. X-ray intensity data were collected on a Bruker APEXII CCD area detector employing graphite-monochromated Mo Kα radiation (λ = 0.71073 Å) at a temperature of 100(1) K. In all cases, rotation frames were integrated using SAINT,[42] producing a listing of unaveraged F^2 and $\sigma(F^2)$ values that were then passed to the SHELXTL[43] program package for further processing and structure solution on a Dell Pentium 4 computer. The intensity data were corrected for Lorentz and polarization effects and for absorption using TWINABS[44] or SADABS.[45] The structures were solved by direct methods (SHELXS-97).[46] Refinement was by full-matrix least squares based on F^2 using SHELXL-97.[46] All reflections were used during refinements. Non-hydrogen atoms were refined anisotropically, and hydrogen atoms were refined using a riding model.

Percent Buried Volume Calculations. Samb*V*ca was used to calculate the percent buried volume ($\%V_{Bur}$) for each complex.[21] The amine atom N(4) in each structure (see Figures 2 and 3) was designated as the atom coordinated to the metal, and the Ti(1)−N(4) distance in each complex was designated as the distance from the center of the sphere (2.28 Å for **1** and 3.07 Å for **2**). The calculations used the following parameters: sphere radius, 3.5 Å; mesh spacing, 0.05 Å; H atoms included; Bondi radii scaled by 1.17.

Synthesis of {Ti[((2-$^tBuNO)C_6H_4CH_2)_3N$]}Cl (1). To a stirred THF solution (15 mL) of $TiCl_4(THF)_2$ (0.303 g, 0.907 mmol, 1 equiv) was added a THF solution (15 mL) of $H_3TriNOx$ (0.500 g, 0.911 mmol, 1.0 equiv) and Et_3N (0.51 mL, 3.7 mmol, 4.0 equiv) dropwise at −78 °C. Stirring was continued at −78 °C for 1 h. The reaction mixture was then warmed to room temperature and was stirred at that temperature for 22 h. Workup was performed in air. The resulting solid precipitate was isolated by vacuum filtration and rinsed with THF. The filtered solid was dissolved in DCM and added to a

separatory funnel with distilled water to remove Et_3N·HCl. The organic layer was extracted three times with DCM, and the combined organic portions were dried under reduced pressure to yield a crude yellow solid. Complex **1** was isolated as yellow crystals by layering Et_2O onto a saturated DCM solution at 0 °C. Yield: 0.302 g, 52.9%. X-ray-quality crystals of **1** were obtained by cooling a saturated DCM solution of **1** to −25 °C. Anal. Calcd for $C_{33}H_{45}ClN_4O_3Ti$: C, 63.01; H, 7.21; N, 8.91. Found: C, 62.76; H, 7.56; N, 8.91. FT-IR (KBr, cm^{-1}): 3326, 2976, 2940, 1959, 1601, 1488, 1456, 1397, 1367, 1314, 1278, 1261, 1235, 1220, 1174, 1117, 1033, 1003, 965, 946, 876, 856, 838, 799, 782, 763, 730, 697, 642, 629, 617, 561, 544, 524. ^1H NMR (300 MHz, $CDCl_3$): δ 7.89 (1 H, d, J = 6.6 Hz, Ar-*H*), 7.45−7.34 (3 H, m, Ar-*H*), 4.60 (1 H, d, J = 12.6 Hz, −CH*H*−), 4.12 (1 H, d, J = 12.6 Hz, −C*H*H−), 0.84 (9 H, s, −C$(CH_3)_3$). ^{13}C NMR (75.4 MHz, $CDCl_3$): δ 143.3 (Ar-*C*), 133.9 (Ar-*C*), 132.6 (Ar-*C*), 129.8 (Ar-*C*), 129.6 (Ar-*C*), 129.4 (Ar-*C*), 67.5 (−CH_2−), 59.9 (−$C(CH_3)_3$), 27.0 (−C$(CH_3)_3$). HRMS (ESI): m/z calcd for $C_{33}H_{45}N_4O_3Ti$, $[1 − Cl]^-$ 593.2971, found 593.2975.

Synthesis of $[((2-^tBuNO)C_6H_4CH_2)_3N]TiF$ (2). A vial with complex **1** (0.0408 g, 0.0645 mmol, 1 equiv) and AgF (0.0403 g, 0.317 mmol, 4.9 equiv) was cooled to −25 °C. In the vial was quickly placed 1.5 mL of −25 °C MeCN. The reaction mixture was briefly stirred and then placed in the dark at −25 °C for 20 h, after which time X-ray-quality crystals of **2** had formed. The products were filtered and washed with −25 °C MeCN and then hexanes. Complex **2** was quickly (to mitigate oxidation of **2** by AgCl and unreacted AgF) rinsed into a clean vial with THF and dried under reduced pressure. Complex **2** was isolated as a pure yellow-orange powder by redissolving the dried solid in Et_2O, filtering, and drying under reduced pressure. Yield: 0.0231 g, 58.1%. Anal. Calcd for $C_{33}H_{45}FN_4O_3Ti$: C, 64.70; H, 7.40; N, 9.15. Found: C, 64.65; H, 7.53; N, 9.04. FT-IR (KBr, cm^{-1}): 3370, 3061, 2969, 2932, 2799, 2719, 1959, 1597, 1582, 1483, 1460, 1448, 1392, 1367, 1358, 1307, 1259, 1231, 1185, 1125, 1114, 1092, 1051, 1039, 1032, 1016, 986, 956, 932, 892, 861, 839, 795, 781, 759, 743, 707, 659 (vs, Ti−F), 636, 619, 602, 581, 560, 539, 521, 503, 488. ^1H NMR (300 MHz, CD_2Cl_2): δ 7.42 (1 H, d, J = 8.1 Hz, Ar-*H*), 7.30−7.21 (2 H, m, Ar-*H*), 7.17−7.12 (1 H, m, Ar-*H*), 4.25 (1 H, d, J = 12.0 Hz, −CH*H*−), 2.69 (1 H, d, J = 12.0 Hz, −C*H*H−), 0.79 (9 H, s, −C$(CH_3)_3$). ^{13}C NMR (75.4 MHz, CD_2Cl_2): δ 148.9 (Ar-*C*), 133.6 (Ar-*C*), 133.3 (Ar-*C*), 128.3 (Ar-*C*), 128.0 (Ar-*C*), 126.6 (Ar-*C*), 66.2 (−CH_2−), 60.7 (−$C(CH_3)_3$), 26.8 (−C$(CH_3)_3$). ^{19}F NMR (282.2 MHz, CD_2Cl_2): δ 114.6.

Fluorine Transfer Reactions. *Triphenylmethyl Fluoride.* The "General Procedure for Fluorine Transfer Reactions" was followed using 1.4 equiv of triphenylmethyl hexafluorophosphate (42% conversion) or 2 equiv of triphenylmethyl bromide (98% conversion) as substrates. $^{19}F\{^1H\}$ NMR (282 MHz, THF): δ − 126.2.

Trimethylsilyl Fluoride. The "General Procedure for Fluorine Transfer Reactions" was followed, except that 2 equiv of a stock solution of the substrate trimethylsilyl chloride (0.1 M in THF) was added in air (98% conversion). $^{19}F\{^1H\}$ NMR (282 MHz, THF): δ −157.1.

Benzoyl Fluoride. The "General Procedure for Fluorine Transfer Reactions" was followed, except that 2 equiv of a stock solution of the substrate benzoyl chloride (0.1 M in THF) was added under N_2 (18% conversion). $^{19}F\{^1H\}$ NMR (282 MHz, THF): δ 17.2.

4-Methylbenzenesulfonyl Fluoride. The "General Procedure for Fluorine Transfer Reactions" was followed using 2 equiv of 4-methylbenzenesulfonyl chloride as a substrate (4% conversion). $^{19}F\{^1H\}$ NMR (282 MHz, THF): δ 66.4.

■ ASSOCIATED CONTENT

Ⓢ Supporting Information

The Supporting Information is available free of charge on the ACS Publications website at DOI: 10.1021/acs.inorg-chem.5b01687.

Computational details, ^1H, ^{13}C, and ^{19}F NMR data, ^1H and ^{19}F VT-NMR data, electrochemical data, DFT-

optimized coordinates for$\{[(HNCH_2CH_2)_3N]Ti\}^+$ and $[(HNCH_2CH_2)_3N]TiF$ in the gas phase, and DFT-optimized coordinates for $\mathbf{1}^+$ and $\mathbf{2}$ in the gas phase, benzene, chloroform, and acetonitrile (PDF)
Crystallographic data for compound **1** (CIF)
Crystallographic data for compound **2** (CIF)

■ AUTHOR INFORMATION

Corresponding Author
*E-mail for E.J.S.: schelter@sas.upenn.edu.

Notes
The authors declare no competing financial interest.

■ ACKNOWLEDGMENTS

■ REFERENCES

(1) Isanbor, C.; O'Hagan, D. *J. Fluorine Chem.* **2006**, *127*, 303−319.
(2) Müller, K.; Faeh, C.; Diederich, F. *Science* **2007**, *317*, 1881−1886.
(3) Campbell, M. G.; Ritter, T. *Org. Process Res. Dev.* **2014**, *18*, 474−480.
(4) Neumann, C. N.; Ritter, T. *Angew. Chem., Int. Ed.* **2015**, *54*, 3216−3221.
(5) Williams, U. J.; Robinson, J. R.; Lewis, A. J.; Carroll, P. J.; Walsh, P. J.; Schelter, E. J. *Inorg. Chem.* **2014**, *53*, 27−29.
(6) Yin, H.; Lewis, A. J.; Williams, U. J.; Carroll, P. J.; Schelter, E. J. *Chem. Sci.* **2013**, *4*, 798−805.
(7) Yin, H.; Lewis, A. J.; Carroll, P.; Schelter, E. J. *Inorg. Chem.* **2013**, *52*, 8234−8243.
(8) Yin, H.; Robinson, J. R.; Carroll, P. J.; Walsh, P. J.; Schelter, E. J. *Chem. Commun.* **2014**, *50*, 3470−3472.
(9) Bogart, J. A.; Lippincott, C. A.; Carroll, P. J.; Schelter, E. J. *Angew. Chem., Int. Ed.* **2015**, *54*, 8222−8225.
(10) Mitzel, N. W.; Parsons, S.; Blake, A. J.; Rankin, D. W. H. *J. Chem. Soc., Dalton Trans.* **1996**, 2089−2093.
(11) Wieghardt, K.; Tolksdorf, I.; Weiss, J.; Swiridoff, W. *Z. Anorg. Allg. Chem.* **1982**, *490*, 182−190.
(12) Mahanthappa, M. K.; Cole, A. P.; Waymouth, R. M. *Organometallics* **2004**, *23*, 836−845.
(13) Mahanthappa, M. K.; Huang, K.-W.; Cole, A. P.; Waymouth, R. M. *Chem. Commun.* **2002**, 502−503.
(14) Hughes, D. L.; Jimenez-Tenorio, M.; Leigh, G. J.; Walker, D. G. *J. Chem. Soc., Dalton Trans.* **1989**, 2389−2395.
(15) Dove, A. P.; Xie, X.; Waymouth, R. M. *Chem. Commun.* **2005**, 2152−2154.
(16) Willner, A.; Niemeyer, J.; Mitzel, N. W. *Dalton Trans.* **2009**, 4473−4480.
(17) Schröder, K.; Haase, D.; Saak, W.; Beckhaus, R.; Kretschmer, W. P.; Lützen, A. *Organometallics* **2008**, *27*, 1859−1868.
(18) Huang, K.-W.; Han, J. H.; Cole, A. P.; Musgrave, C. B.; Waymouth, R. M. *J. Am. Chem. Soc.* **2005**, *127*, 3807−3816.
(19) Barroso, S.; Madeira, F.; Calhorda, M. J.; Ferreira, M. J.; Duarte, M. T.; Martins, A. M. *Inorg. Chem.* **2013**, *52*, 9427−9439.
(20) Majumdar, S.; Stauber, J. M.; Palluccio, T. D.; Cai, X.; Velian, A.; Rybak-Akimova, E. V.; Temprado, M.; Captain, B.; Cummins, C. C.; Hoff, C. D. *Inorg. Chem.* **2014**, *53*, 11185−11196.
(21) Poater, A.; Cosenza, B.; Correa, A.; Giudice, S.; Ragone, F.; Scarano, V.; Cavallo, L. *Eur. J. Inorg. Chem.* **2009**, *2009*, 1759−1766.
(22) Clavier, H.; Nolan, S. P. *Chem. Commun.* **2010**, *46*, 841−861.
(23) Maity, A. K.; Fortier, S.; Griego, L.; Metta-Magaña, A. J. *Inorg. Chem.* **2014**, *53*, 8155−8164.
(24) Conley, M. P.; Forrest, W. P.; Mougel, V.; Copéret, C.; Schrock, R. R. *Angew. Chem., Int. Ed.* **2014**, *53*, 14221−14224.
(25) Thangavel, A.; Wieliczko, M.; Bacsa, J.; Scarborough, C. C. *Inorg. Chem.* **2013**, *52*, 13282−13287.
(26) Connelly, N. G.; Geiger, W. E. *Chem. Rev.* **1996**, *96*, 877−910.
(27) Christe, K. O.; Wilson, W. W.; Wilson, R. D.; Bau, R.; Feng, J. A. *J. Am. Chem. Soc.* **1990**, *112*, 7619−7625.
(28) Herzog, A.; Liu, F.-Q.; Roesky, H. W.; Demsar, A.; Keller, K.; Noltemeyer, M.; Pauer, F. *Organometallics* **1994**, *13*, 1251−1256.
(29) Kuehnel, M. F.; Holstein, P.; Kliche, M.; Krüger, J.; Matthies, S.; Nitsch, D.; Schutt, J.; Sparenberg, M.; Lentz, D. *Chem. - Eur. J.* **2012**, *18*, 10701−10714.
(30) Rioux, F.; Schmidt, M. W.; Gordon, M. S. *Organometallics* **1997**, *16*, 158−162.
(31) Nikiforov, G. B.; Roesky, H. W.; Koley, D. *Coord. Chem. Rev.* **2014**, *258−259*, 16−57.
(32) Santamaría, C.; Beckhaus, R.; Haase, D.; Saak, W.; Koch, R. *Chem. - Eur. J.* **2001**, *7*, 622−626.
(33) Burk, M. J.; Staley, D. L.; Tumas, W. *J. Chem. Soc., Chem. Commun.* **1990**, 809−810.
(34) Fout, A. R.; Scott, J.; Miller, D. L.; Bailey, B. C.; Pink, M.; Mindiola, D. J. *Organometallics* **2009**, *28*, 331−347.
(35) Piglosiewicz, I. M.; Kraft, S.; Beckhaus, R.; Haase, D.; Saak, W. *Eur. J. Inorg. Chem.* **2005**, *2005*, 938−945.
(36) Grün, M.; Harms, K.; Köcker, R. M. Z.; Dehnicke, K.; Goesmann, H. *Z. Anorg. Allg. Chem.* **1996**, *622*, 1091−1096.
(37) Haiges, R.; Boatz, J. A.; Schneider, S.; Schroer, T.; Yousufuddin, M.; Christe, K. O. *Angew. Chem., Int. Ed.* **2004**, *43*, 3148−3152.
(38) Shah, S. A. A.; Dorn, H.; Gindl, J.; Noltemeyer, M.; Schmidt, H.-G.; Roesky, H. W. *J. Organomet. Chem.* **1998**, *550*, 1−6.
(39) Taw, F. L.; Clark, A. E.; Mueller, A. H.; Janicke, M. T.; Cantat, T.; Scott, B. L.; Hay, P. J.; Hughes, R. P.; Kiplinger, J. L. *Organometallics* **2012**, *31*, 1484−1499.
(40) Manxzer, L. E.; Deaton, J.; Sharp, P.; Schrock, R. R. *Inorg. Synth.* **1982**, *21*, 135−140.
(41) Thomson, R. K.; Scott, B. L.; Morris, D. E.; Kiplinger, J. L. *C. R. Chim.* **2010**, *13*, 790−802.
(42) *SAINT*; Bruker AXS Inc., Madison, WI, 2009.
(43) *SHELXTL*; Bruker AXS Inc., Madison, WI, 2009.
(44) Sheldrick, G. M. *TWINABS*; University of Göttingen, Göttingen, Germany, 2008.
(45) Sheldrick, G. M. *SADABS*; University of Göttingen, Göttingen, Germany, 2007.
(46) Sheldrick, G. M. *Acta Crystallogr., Sect. A: Found. Crystallogr.* **2008**, *64*, 112−122.